



# Time-Temperature Dependent Response of Filament Wound Composites for Flywheel Rotors

John C. Thesken  
Ohio Aerospace Institute, Brook Park, Ohio

Cheryl L. Bowman and Steven M. Arnold  
Glenn Research Center, Cleveland, Ohio

Richard C. Thompson  
University of Texas at Austin, Austin, Texas

## The NASA STI Program Office . . . in Profile

Since its founding, NASA has been dedicated to the advancement of aeronautics and space science. The NASA Scientific and Technical Information (STI) Program Office plays a key part in helping NASA maintain this important role.

The NASA STI Program Office is operated by Langley Research Center, the Lead Center for NASA's scientific and technical information. The NASA STI Program Office provides access to the NASA STI Database, the largest collection of aeronautical and space science STI in the world. The Program Office is also NASA's institutional mechanism for disseminating the results of its research and development activities. These results are published by NASA in the NASA STI Report Series, which includes the following report types:

- **TECHNICAL PUBLICATION.** Reports of completed research or a major significant phase of research that present the results of NASA programs and include extensive data or theoretical analysis. Includes compilations of significant scientific and technical data and information deemed to be of continuing reference value. NASA's counterpart of peer-reviewed formal professional papers but has less stringent limitations on manuscript length and extent of graphic presentations.
- **TECHNICAL MEMORANDUM.** Scientific and technical findings that are preliminary or of specialized interest, e.g., quick release reports, working papers, and bibliographies that contain minimal annotation. Does not contain extensive analysis.
- **CONTRACTOR REPORT.** Scientific and technical findings by NASA-sponsored contractors and grantees.

- **CONFERENCE PUBLICATION.** Collected papers from scientific and technical conferences, symposia, seminars, or other meetings sponsored or cosponsored by NASA.
- **SPECIAL PUBLICATION.** Scientific, technical, or historical information from NASA programs, projects, and missions, often concerned with subjects having substantial public interest.
- **TECHNICAL TRANSLATION.** English-language translations of foreign scientific and technical material pertinent to NASA's mission.

Specialized services that complement the STI Program Office's diverse offerings include creating custom thesauri, building customized databases, organizing and publishing research results . . . even providing videos.

For more information about the NASA STI Program Office, see the following:

- Access the NASA STI Program Home Page at <http://www.sti.nasa.gov>
- E-mail your question via the Internet to [help@sti.nasa.gov](mailto:help@sti.nasa.gov)
- Fax your question to the NASA Access Help Desk at 301-621-0134
- Telephone the NASA Access Help Desk at 301-621-0390
- Write to:  
NASA Access Help Desk  
NASA Center for Aerospace Information  
7121 Standard Drive  
Hanover, MD 21076



# Time-Temperature Dependent Response of Filament Wound Composites for Flywheel Rotors

John C. Thesken  
Ohio Aerospace Institute, Brook Park, Ohio

Cheryl L. Bowman and Steven M. Arnold  
Glenn Research Center, Cleveland, Ohio

Richard C. Thompson  
University of Texas at Austin, Austin, Texas

Prepared for the  
14th Symposium on Composite Materials: Testing and Design  
sponsored by the American Society for Testing and Materials  
Pittsburgh, Pennsylvania, March 11–12, 2002

National Aeronautics and  
Space Administration

Glenn Research Center

## Acknowledgments

This work was supported by NASA Glenn Research Center's Rotor-Safe Life Program under the direction of Kerry McLallin and J. Rodney Ellis. Material testing and characterization were conducted with the technical assistance of Christopher Burke, Linda McCorkle, and Linda Inghram. The authors thank Gary Roberts for valuable discussions and Jayaraman Raghavan for providing AS4/3501-6 data files. This work received special recognition from NASA by way of a "2002 Space Flight Awareness Team Award" for outstanding support given to the Rotor Safe Life Program in developing a basic understanding of time-dependent behavior of pre-loaded composite flywheel rotors for the International Space Station.

Trade names or manufacturers' names are used in this report for identification only. This usage does not constitute an official endorsement, either expressed or implied, by the National Aeronautics and Space Administration.

Available from

NASA Center for Aerospace Information  
7121 Standard Drive  
Hanover, MD 21076

National Technical Information Service  
5285 Port Royal Road  
Springfield, VA 22100

Available electronically at <http://gltrs.grc.nasa.gov>

# Time-Temperature Dependent Response of Filament Wound Composites for Flywheel Rotors

John C. Thesken  
Ohio Aerospace Institute  
Brook Park, Ohio 44142

Cheryl L. Bowman and Steven M. Arnold  
National Aeronautics and Space Administration  
Glenn Research Center  
Cleveland, Ohio 44135

Richard C. Thompson  
University of Texas at Austin  
Austin, Texas 78712

## Abstract

Flywheel energy storage offers an attractive alternative to the electrochemical battery systems currently used for space applications such as the International Space Station. Rotor designs utilizing the load carrying capacity of carbon fibers wound in the hoop direction are capable of high operational speeds and specific energies. However, the long-term durability of such rotors may be limited by the time-temperature dependent behavior of the epoxy matrix which controls the uniaxial properties transverse to the fiber and the shear properties. This proposition was investigated for the prototypical rotor material, IM7/8552. Flat filament wound panels were made using the same process as for composite rotors. Coupon specimens, sectioned normal and parallel to the winding axis, were tested in compression and tension, at room temperature (RT), 95 °C and 135 °C for strain rates from  $5 \times 10^{-6}/s$  to  $5 \times 10^{-3}/s$ . Creep and stress relaxation testing ran 72 hrs followed by a 72 hr recovery. Time, temperature and load sign dependent effects were significant transverse to the fiber. Under a fixed deformation of  $-0.5\%$  strain for 72 hrs, compressive stresses relaxed 16.4% at 135 °C and 13% at 95 °C. Tensile stresses relaxed only 7% in 72 hrs at 135 °C for 0.5% strain. The postulate of a linear hereditary material response and the application of Boltzmann's principle of superposition to describe the behavior observed here are problematic if not intractable. Undoubtedly microstructural analysis including the influence of residual stresses due to processing will be needed to resolve the observed paradoxes. Within the scope of these experiments, uniaxial compressive stress relaxation data may be used to bound the amount of relaxation with time of radial pre-load stresses in flywheel rotors. A more detailed appraisal of the design implications of these results is made in the analysis by Saleeb and co-workers [1].

## Introduction

Successful space flight operations require onboard power management systems that reliably achieve mission objectives for a minimal launch weight. For power systems that

utilize electrochemical batteries, flywheel energy storage is an attractive alternative. Flywheels can attain relatively greater power and energy densities with no fall-off in capacity under repeated charge-discharge cycles. However, the implementation of several flywheel designs considered for space applications requires the safe-life qualification of the technology enabling rotor material: carbon fiber reinforced polymer composite.

Specifics of flywheel design and the evolution of composites for rotor materials may be traced through a number of comprehensive state-of-the-art reviews [2–6]. Examples of material system selections for flywheel devices are given in Genta [2] and DeTeresa [4] whereas optimization for integrated system design is given by Bitterly [5]. Fundamentally rotor designs utilizing the high specific strength of carbon fibers wound in the hoop direction are capable of high rotational speeds and specific energies. However, as pointed out by DeTeresa [4], this configuration exposes the weaker, matrix dominated, properties transverse to the fiber to the problem of tensile radial stresses.

This problem has evolved rotor/hub solutions that induce compressive radial stresses acting transverse to the fiber; they are categorized into three design topologies: 1) compression preloaded rotor, 2) growth matching hub and 3) mass loaded inner rim. These configurations pose an interesting family of analytical problems to determine the elastic stress and deformation state. The analytical model must be capable of simulating: single/multiple, annular/solid, and anisotropic/isotropic disk systems, subjected to pressure surface tractions, body forces and interfacial misfits. In [6], Arnold and co-workers have developed such a model; it has been used to determine the key design variables and their associated influence through an extensive parametric study. In general the important parameters were shown to be misfit, mean radius, thickness, material property and/or load gradation, and speed. Clearly the performance and long-term durability of a carbon-fiber polymer rotor depends upon the stability of several dimensions that are transverse to the winding filaments.

In the case of flywheel systems, manufactured with a pre-load or strain-matching design in mind,<sup>1</sup> time-temperature dependent material behavior may have a significant life-limiting impact. Loss of pre-load or a change in the induced strain state over time would induce disk separation and lead to loss of function of the system. Concerns with the time-temperature dependent behavior of composite flywheel rotors have been raised by several previous researchers [7–10]. Tzeng [7,8] has developed viscoelastic solutions for thick walled cylinders while accounting for ply-by-ply variations of rotor structural properties. Emerson and Bakis [9] have made experimental investigations of interference-fitted composite rings; ring materials included carbon/epoxy, glass/epoxy and aluminum. This data was later analyzed by Emerson and Bakis using a viscoelastic model [10]. While fundamentally viscoelasticity may be a useful representation of the matrix dominated properties it may not be entirely accurate. Consequently, the need to assess and classify the constitutive behavior of the carbon fiber composite utilized in a given design is of utmost importance. This is the objective of the experimental investigation described here.

---

<sup>1</sup>A pre-loaded flywheel is composed of a number of concentric rings (be they disk or logs) press-fit together with a specified misfit between each ring. Therefore, the resulting laminated flywheel has a compressive radial stress at the interface of each concentric ring.

This work was initiated within the Rotor Safe-Life Program in support of the Flywheel Energy Storage System (FESS) effort at the NASA Glenn Research Center. FESS is evaluating pre-loaded concentric ring rotors made of wound IM7 carbon fiber and 8552 epoxy prepreg tapes. The rotor design and development work is being done at the University of Texas Center for Electromechanics (UTCEM); this includes a variety of structural element testing procedures developed by UTCEM that examine burst criteria [11] and long term time-temperature dependent deformations. The objective of the experimental work made within the Rotor Safe-Life Program was to evaluate material performance issues at the coupon level. This data would then be used in conjunction with structural element testing to develop lifing methodologies and material qualification procedures. It is anticipated that coupon level testing and improved lifing methods could reduce structural element test requirements and accelerate the development of new rotor designs. Thus far, the impact of these coupon specimen results on flywheel rotor design has been investigated and reported in a related paper by Saleeb et al. [1].

## Experimental Approach

The time-temperature dependent nature of polymers and their composites, e.g., carbon fiber reinforced epoxy, have been widely investigated [12–19]. Recent studies that examine the applicability of viscoelastic and viscoplastic theoretical frameworks may be found by Raghavan and Meshi [20] and Al-Haik and co-workers [21]. These works and the experimental methods applied by Arnold et al. [22] guided the research presented in this paper.

Typically, three types of experimentation are necessary to support the rational formulation of constitutive equations for high temperature structural systems. These are: 1) exploratory tests which guide the development of theory and test the fundamental concepts embedded in the theoretical framework; 2) characterization tests which provide the required data base for determining the specific functional forms and material parameters to represent a particular material over a given range of conditions; and 3) verification tests, often prototypical in nature, which provide the ultimate test of a constitutive model through comparison of structural response with predictions based on the model. Results from verification tests ideally provide feed back for subsequent constitutive model development efforts. The present work will focus primarily upon *coupon-level tests of the exploratory* type. The fundamental concepts that will be tested are outlined below beginning with the notion of linear hereditary constitutive behavior transverse to the fiber and the issue of a recoverable initial stress/strain state.

Linearity holds when the time dependent relaxation modulus or the creep compliance data determined from stress relaxation and creep tests are independent of the amplitude of the applied deformation or stress. The eventual recovery of the initial stress/strain state when the applied deformation or stresses are returned to zero indicates the absence of permanent straining and/or damage. Defining the existence and applicability bounds for such linear hereditary response is valuable to design engineers seeking to use Boltzmann's principle of superposition to predict the long term uniaxial stress/strain response of the material.

Temperature reflects the energy available for molecular motion of the polymer and like time, is a parameter of the constitutive response. Higher temperatures ease the rearrangement of the polymer chain backbones thereby manifesting greater compliance

and shorter relaxation times. Indeed, relaxation times are often found to scale with temperature giving rise to the time-temperature superposition principle (TTSP). Master relaxation modulus curves and master creep compliance curves may be constructed over a wide range of time by shifting multiple temperature data to a specific reference temperature. Note at the glass transition temperature,  $T_g$ , a significant change in the degree of molecular motion occurs as the polymer transforms from the glassy state to the rubbery state. Hence the nature of the shift factor also changes. Necessarily operation temperatures for carbon fiber epoxy rotors are expected to be less than  $T_g$ . Dynamic Mechanical Analysis (DMA) was made to determine the glass transition temperature and all mechanical testing was made at lower temperatures than  $T_g$ .

The test program consisted primarily of isothermal monotonic loading tests and isothermal stress relaxation tests and creep tests. Mechanical response to compressive and tensile loading was examined to determine the level of complexity required of the macro-level constitutive model, in particular, the number and type of stress invariants in the object function for the model. Under monotonic loading, coupons were tested at different strain rates to provide the first indications of time-temperature dependent stress-strain response. Temperature and either strain or stress respectively are held constant in the stress relaxation tests or creep tests. While neither of these variables is expected to be constant during normal operation, prototypical experiments were made to identify possible synergistic effects due to cyclic loads. Details of the experimental procedures follow.

#### *Flat Coupon Specimen Manufacturing*

Hexcel IM7/8552 in the form of pre-impregnated tow was used to wind flat specimen panels. The 8552 resin system is an amine cured toughened epoxy. Neat resin has a dry  $T_g$  of 200 °C when cured at 177 °C. Properties of the 8552 neat resin and IM7 carbon fibers are given in Table 1.

Table 1—*Composite constituent properties*

Material	Density (g/cc)	Tensile Modulus (kN/mm <sup>2</sup> )	Tensile Strength (N/mm <sup>2</sup> )	Tensile strain-to-failure (%)
8552	1.30	4.67	120	1.7
IM7	1.77	276	5379	1.8

Flat panels, were manufactured on a 35.56 cm square steel hollow mandrel, with a wall thickness of about 0.95 cm. Individual pre-impregnated tow, under about 35 N tension, was wound onto the mandrel surface to create a square cylinder. Tow advance was about 89.8°, resulting in a slight tow-to-tow overlap. Specifications for the IM7/8552 tow included a bandwidth of about 0.32 cm with an approximate resin content of 60%. After achieving the finished thickness, the part was prepared for curing using caul plates on the outside surface of the material and conventional vacuum bagging procedures. Placed in an autoclave, the part was cured at 177 °C using the cure cycle specified by the material supplier [23].

The four-sided cured part was then machined into separate panels using diamond cutoff tooling. Efforts were made to preserve the filament winding orientation, i.e., sectioned panels reflect tow advance. Residual strains are present in the composite panels, in the direction of the carbon fiber. This residual strain is thought to be associated with the tension induced in the fiber direction due to mandrel thermal expansion during cure and the winding tension applied to the tow. During mandrel expansion, prior to resin staging, the fibers facing closest to the mandrel surface carry more of the mandrel expansion load. After cure, this strain profile, with the relative tensile fiber strain maximum at the inner panel surface and decreasing toward the outer surface, is believed to be responsible for a slight convex warp of the panels.

Prior to specimen machining, panels were subjected to ultrasonic examination to produce C-scan representations of the material quality. The same nondestructive evaluation methods were used as those being used by Baaklini and co-workers [24] for flywheel certification. Compaction attributes of flat panel and hoop wound rotors, such as void content and fiber volume fraction, were found to be similar. Coupon specimens were sectioned from the flat panels using diamond saw. Specimen edges were then lightly sanded with fine grit paper to remove any cutting marks. Specimen geometries were in accordance with ASTM Test Method for Tensile Properties of Polymer Matrix Composite Materials (D3039). The plan geometry for each specimen was 25.4 x 190.6 mm. The nominal specimen thickness was about 2.82 mm. After machining specimens were dried in vacuum at 115 °C for 48 hrs and stored in a dessicator during final preparation before testing. Pull tabs were cut from prefabricated sheets of GRFP. These were then tapered and bonded to the ends of the specimen using the 3M structural adhesive AF 163–2L. The epoxy adhesive was cured following manufacturers guideline.

The specimens were strain gaged as suggested in ASTM D 3039 and in ASTM Test Method for Compressive Properties of Polymer Matrix Composite Materials with Unsupported Gage Section by Shear Loading (D3410) so that specimen bending could be monitored. Sullivan [15] provides some useful guidelines on the use of strain gages in creep tests of polymer composites but special considerations are still needed for long term testing at elevated temperature. This is particularly so with respect to tests made transverse to the reinforcement fiber. Here the polymeric film backing materials may undergo creep while the metallic foil may have a local reinforcement effect. These issues were discussed with Prof. J. Raghavan<sup>2</sup> who used MicroMeasurement WK-type gages in creep tests of AS4/3501-6 carbon fiber epoxy at temperatures up to 200 °C [20]. In that work, the stability of the WK-type gage was verified by bonding them to stainless steel samples and subjecting them to elevated temperatures and stress over the same duration as the creep tests. In the case of errors caused by strain gage reinforcement, Perry [25,26] suggests that 7 kN/mm<sup>2</sup> is the lower modulus limit for the application of foil strain gages to low modulus material. Sullivan [15] found that the error is about 6% for materials with a modulus of 4 kN/mm<sup>2</sup> and this error will decrease with increasing modulus of the base material. Strain gage reinforcement effects are probably negligible for IM7/8552 which is expected to have a transverse modulus of greater than 7 kMN/mm<sup>2</sup>. With this in mind WK-type gages were selected for use in experiments

---

<sup>2</sup>Personal communication with Prof. J. Raghavan, U. of Manitoba, Dept. of Mechanical & Industrial Engineering, 348D Engineering Building, 15 Gillson Street, Winnipeg, MB R3T 5V6, Canada.

made at elevated temperature. Room temperature tests were made with CEA-type gages. Gage bonding practices followed manufacturer's recommendations.

Thermal stress effects and stability at temperature were examined by heating unconstrained gaged specimens and observing the stress free gage output as a function of time and temperature. During the tests, elongation was also measured on one edge of the specimen using an axial extensometer.

### *Test Set-up*

Elevated temperatures were achieved using a custom made radiant mini-furnace. Closed-loop temperature control was provided through a reference thermocouple attached to a fixed position in the furnace. Calibration of the specimen temperature and verification of thermal gradients was accomplished by heating a specimen instrumented with a series of vertical and horizontal embedded thermocouples. Calibration factors were determined for each test temperature. Through careful adjustments of oven position and placement of insulation it was possible to reduce the thermal gradients in the center measurement region of the specimen to be less than 0.3 °C/mm.

Mechanical testing was performed on a computer controlled MTS servo-hydraulic test frame. In addition to back-to-back foil strain gages used to monitor bending strains, an edge-mounted extensometer with a 12.7 mm gage length was used to measure deformations. Previous examples of compressive creep or stress relaxation tests transverse to the fiber direction have used special test fixtures and anti-buckling guides [12,13,16]. The tests made here were in MTS grips aligned to within  $\pm 20 \times 10^{-6}$  strain, without additional support. Based on the specimen geometry and the distance between grips, Euler buckling calculations were made to determine the maximum loads or deformations that could be applied without the occurrence of instability. For a grip edge to grip edge distance of 54.9 mm and a specimen thickness of 2.82 mm, buckling instability would be expected to occur at a compressive strain of -0.87%. This is assuming the grips may be approximated by fixed end conditions.

A room temperature compressive test was made to verify the stability of the specimen. At an axial strain of -0.88% the bending strains were measured to be only 6.0% of the axial value; buckling instability did not occur. On subsequent reloading to cause compressive failure, bending strains began to exceed 10% of the compressive axial strain when it measured -0.81%. The specimen however was capable of sustaining a maximum compressive strain of -1.65% before the loading capacity dropped off to zero due to buckling. The discrepancy between measurements and Euler's buckling limit may be due to the tabbing material that supported the specimens about an extra 7.5 mm from the grip edges on either end. Note that the Euler equation for a length of 40 mm length gives a buckling strain of about 1.62%. This information was then used to limit the maximum compressive strain and stress levels that could be applied in the tests.

## **Experimental Results and Discussion**

### *Material Characterization*

Fiber volume fraction and void contents were determined in accordance with ASTM Test Method for Fiber Content of Resin Matrix Composites by Matrix Digestion

(D 3171) and ASTM Test Method for Void Content of Reinforced Plastics D2734. A typical range of values for a panel of this material are: fiber volume fraction in the range of 56.6–57.15% and void content range of 1.4%–0.3%.

The dynamic shear moduli were measured following the ASTM Test Method for Assignment of the Glass Transition Temperature by Dynamic Mechanical Analysis (E 1640). The tests were made using an ARES unit manufactured by Rheometrics Scientific As received material and a sample aged for 72 hrs at 135 °C were tested to ascertain the potential for chemical aging during testing at elevated temperature. The specimen size was 29.6 x 10.3 x 2.8 mm with the fibers oriented in the direction transverse to the axis of rotation. The specimen was deformed in torsion at a fixed frequency of 10 radians per second to a strain of 0.15% The applied deformation function is sinusoidal so the maximum strain rate for the experiment is 1.5%/s, the product of frequency and strain amplitude. The shear storage modulus ( $G'$ ) and shear loss modulus ( $G''$ ) were recorded as the specimen was heated to 300 °C at a rate of 5 °C per minute. The shear moduli  $G'$  and  $G''$  are shown as a function of temperature (Figure 1); two vertical dashed lines delineate the glassy, transitory, and rubbery regions at these test conditions.

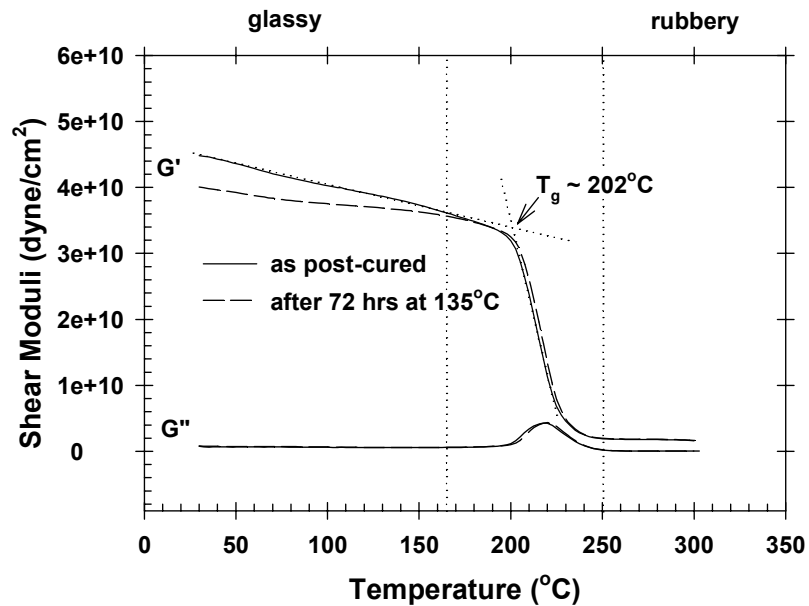


Figure 1.—The storage and loss moduli as a function of temperature measured by dynamic torsion for a specimen with the fibers oriented transverse to the rotation axis.

Using the standard intercept approach on a linear scale the  $T_g$  was determined to be approximately the same for both samples: 202 °C. The measured  $T_g$  agrees well with the manufacturers reported data for this cure/post-cure cycle. Note that the transition region would occur at lower temperatures for slower deformation rates. Further testing will be required to determine if the regime falls as low as 95 °C or 135 °C. The agreement between the  $T_g$  of the as-received sample and the  $T_g$  of the 72 hr aged sample indicates that, with respect to the time and temperatures evaluated here, the composite may be considered as fully cured. Thus chemical aging is not expected to play a role in the time-temperature dependent material behavior reported here.

*Monotonic Testing*

*Longitudinal Properties.*—The tensile elastic properties in the fiber direction are reported since they are relevant to subsequent design investigations. The longitudinal modulus,  $E_L$ , was measured at room temperature for eight different specimens tested at  $10^{-4}$ /s strain rate. The average value measured for  $E_L$  was  $151 \text{ kN/mm}^2 \pm 4.0\%$ . Tests made at  $135 \text{ }^\circ\text{C}$  for strain rates of  $5 \times 10^{-6}$ /s and  $5 \times 10^{-3}$ /s yielded  $E_L$  values of  $155 \text{ kN/mm}^2$  and  $150 \text{ kN/mm}^2$ , respectively. Clearly any variation due to strain rate and elevated temperature is smaller than the specimen-to-specimen variability in the room temperature data. The Rule of Mixture predicts values for  $E_L$  of 158 to  $160 \text{ kN/mm}^2$ , 6% greater than the mean room temperature values. Note that if the matrix was completely discounted the Rule of Mixture prediction would be  $156.2$  and  $157.7 \text{ kN/mm}^2$ , still greater than measured values. The tow-winding angle of  $89.8^\circ$  is too close to  $90^\circ$  to account for the 6% difference between measurements and prediction. Indeed tensor transformation of the orthotropic stiffness coefficients suggest that the winding angle could be decreased to  $86^\circ$  without causing a difference greater than 1%. The discrepancy between modulus data and the prediction is likely related to the accuracy of the volume fraction and/or the constituent properties. The average Poisson’s ratio corresponding to an applied stress in the fiber direction,  $\nu_{LT}$ , was measured to be  $0.30 \pm 0.02$  at room temperature.

*Transverse Properties.*—The average room temperature mechanical properties transverse to the fiber were determined from 5 tests (Table 2) and are listed in the first row. The transverse modulus is defined as  $E_T$  and the Poisson’s ratio corresponding to a deformation in the fiber direction due to a load in the transverse direction is defined as  $\nu_{TL}$ . Tests were made at a displacement rate of  $0.0254 \text{ mm/s}$ . A single tensile test was made at  $135 \text{ }^\circ\text{C}$  to determine the reduction in tensile strength due to elevated temperature. This test was used to guide load levels in tensile creep tests. Note also that the longitudinal and transverse data are consistent with the requirement that the ratios  $\nu_{LT}/E_L$  and  $\nu_{TL}/E_T$  be equal. The composite transverse tensile strength at RT is about 58% of the neat resin tensile strength indicating a considerable knock down in tensile strength due to the presence of reinforcing fibers and fiber/matrix interfaces.

Table 2—*Transverse Material Properties*<sup>a</sup>

Compression $E_T$ ( $\text{kN/mm}^2$ )	Tensile $E_T$ ( $\text{kN/mm}^2$ )	$\nu_{TL}$	Tensile Strength ( $\text{N/mm}^2$ )	Tensile strain-to-failure (%)
$9.69 \pm 0.78$	$9.07 \pm 0.44$	$0.021 \pm 0.002$	$69.2 \pm 13.4$	$0.80 \pm 0.12$
--	8.274	0.017	62.7	0.84

<sup>a</sup>First row data are mean room temperature values; the second row is data for a single  $135 \text{ }^\circ\text{C}$  test

The influence of strain rate on  $E_T$  was studied in a series of monotonic compression and tension tests. The experiments were made in strain control to a maximum strain of 0.3% over a range of strain rates from  $5 \times 10^{-6}$ /s to  $5 \times 10^{-3}$ /s. Test temperatures included RT,  $95^\circ\text{C}$  and  $135 \text{ }^\circ\text{C}$ . Figure 2 shows  $E_T$  as a function of strain rate for the three test temperatures. There were too few tensile  $E_T$ /strain rate data to reveal a distinction between compression and tension.

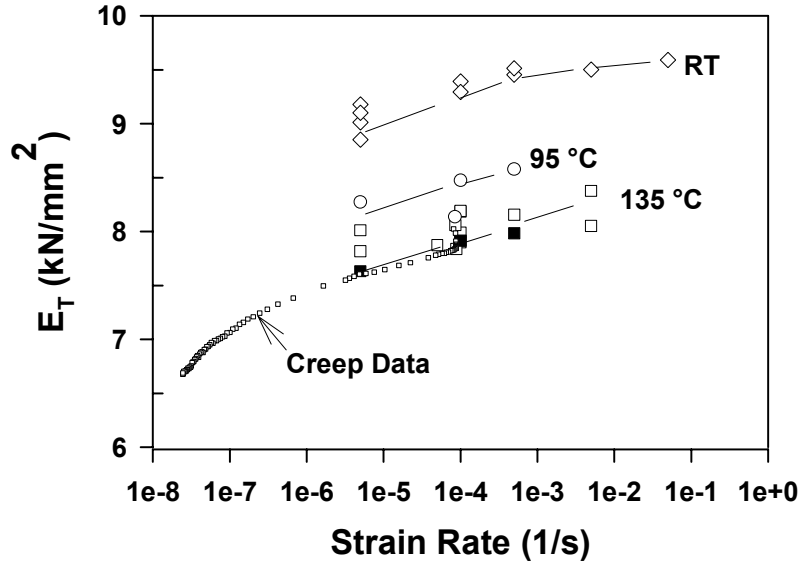


Figure 2.—Elastic Modulus as a function of strain rate, open symbols are compression data, filled boxes are tensile, small squares are converted compressive creep data.

These data give the first indication of the time-temperature dependence of the transverse behavior of IM7/8552.  $E_T$  is seen to increase about 5% over 3 decades of increasing strain rate from  $5 \times 10^{-6}/s$ . The data appear to segregate along curved lines of constant temperature that appear self-similar. The room temperature data are at least 10% greater than the data measured at  $135^\circ\text{C}$ . It is proposed that the time scale for more significant changes in modulus is quite long and becomes apparent at slower strain rates. This is illustrated by plotting the time dependent modulus for a set of compressive creep data at  $135^\circ\text{C}$  as a function of the average strain rate up to that instant in time. The resulting series of modulus/strain rate data are shown in Fig. 2 as the arc of small open squares extending 2 decades less than  $5 \times 10^{-6}/s$ . Over these 2 decades the series of  $E_T$  values decrease 13%. Where the creep based data overlap with the discrete modulus tests made at  $135^\circ\text{C}$ , there is good agreement. As the total strains in these tests are of the order 0.5% this shows that the time scales for time dependent behavior at  $135^\circ\text{C}$  are of the order  $10^4$ s or greater.

#### *Stress Relaxation and Creep Tests*

As described in the experimental procedure, bending strains were closely monitored and all tests reported were within the limits suggested in ASTM D3039 and ASTM D3410. For compression ASTM D3039 recommends that bending strains be less than 10% of the axial strains. A typical plot of the percent bending as a function of axial strains is given for a long-term compression test in Fig. 3; the bending strains were less than  $\pm 5\%$  of the axial strain level.

The magnitude of the applied strain for the tensile and compressive relaxation tests was 0.5%. The magnitude of the applied stress for the tensile and compression creep tests was  $41.4 \text{ N/mm}^2$ . Generally the duration of the applied stress/strain period and the

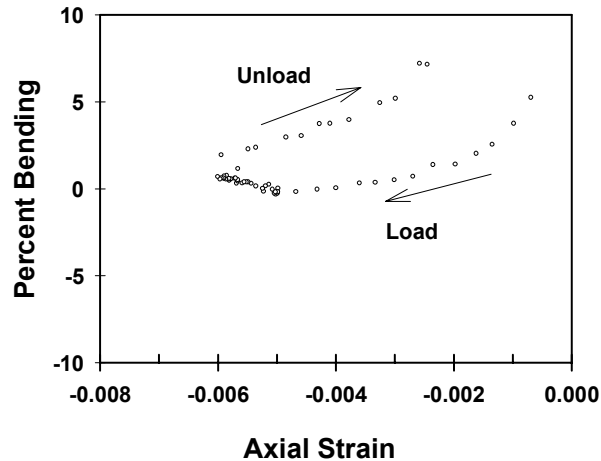


Figure 3.—A typical example of the percent bending strain with respect to axial strains for a creep test.

unstressed /unstrained recovery periods were both intended to be about  $2.6 \times 10^5$ s (72 hrs). Instances where these periods differed are apparent in the plots of the data. The main results of the stress relaxation and creep tests are given in Figs. 4 to 6. The plots show the respective stress and strain responses for each test type as a function of time. For convenient comparison of the tensile and compressive responses, the data are presented as absolute magnitudes. The reader is reminded that the sense of stress for the recovery portion of the stress relaxation plots changes as the control strain approaches zero. This is annotated by the use of filled data symbols to for a tensile stress state and unfilled symbols for a compressive stress state. The influence of tensile and compressive states on stress relaxation response (Fig. 4) and creep response (Fig. 5) is contrasted for tests made at 135°C. The influence of temperature is given in the comparison of compression stress relaxation experiments (Fig. 6) and compression creep experiments (Fig. 7) made at 95 °C and 135 °C.

The creep and stress relaxation tests shown in Figs. 4 to 5 clearly show that the response rate due to compressive stresses or strains is greater than the response rate due to tensile stresses and strains. For example, compressive and tensile stresses relaxed 16.4% and 7% respectively after 72 hrs at a strain magnitude of 0.5% and a temperature of 135 °C. Qualitatively, the tensile stress relaxation and tensile creep straining processes shown in Figs. 4 and 5 appear to have shut down. This is also observed during the stress recovery part of the stress relaxation plots of Fig.4. As the applied compressive strain is removed the stress response becomes tensile and appears to arrest after a small amount of recovery. Alternatively the tensile stress relaxation response that appears to have shut down during the applied tensile strain is seen to be recovering the zero stress state when the applied strain is zero. The stress is compressive during this recovery phase.

The creep data shown in Fig. 5 indicates that tensile creep rates are much slower than compressive creep rates and that tensile creep tests were also prone to creep rupture. This could be expected due to the presence of weak fiber/matrix interfaces already apparent in the 58% knock down in tensile strength with respect to neat resin. Therefore recovery data for the unloaded tensile creep specimens is unavailable. Creep recovery in the compressive

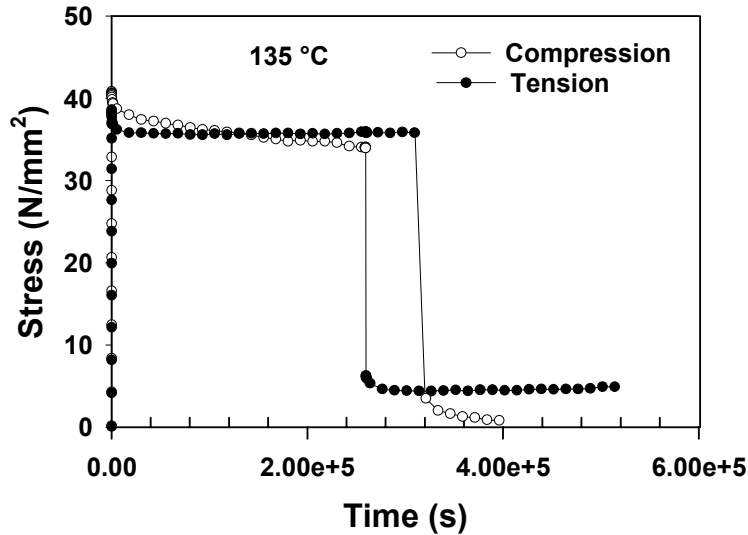


Figure 4.—Tensile and compressive stress relaxation at 135 °C as a function of time. Stress is plotted as absolute value, note that the sense of stress transposes during the recovery portion of the test so that filled symbols are tensile.

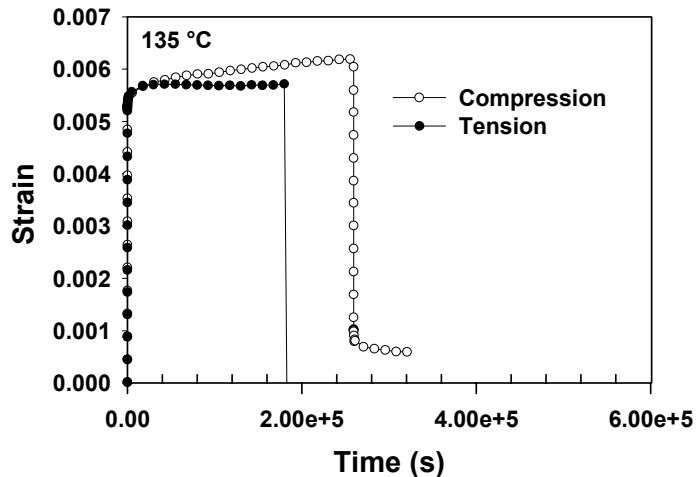


Figure 5.—Tensile and compressive creep at 135 °C as a function of time. Strain is plotted as absolute value. The tensile test failed after 52 hrs.

creep tests were easier to monitor and the rate of recovery was relatively slow with respect to the initial phase of the test.

As expected, reducing the temperature from 135 °C to 95 °C yielded reduced stress relaxation and creep response. For example, compressive stress relaxation was only 13% at 95 °C as compared to 16.4% at 135 °C. The response curves shown in Figs. 6 and 7 are classic examples of the time-temperature dependent material response. Converting the data to time dependent compliance shown in Fig. 8 it is possible to investigate the applicability of the time temperature superposition principle (TTSP). This is accomplished by shifting the 135 °C data to the right so that a master curve covering a longer time range is created at

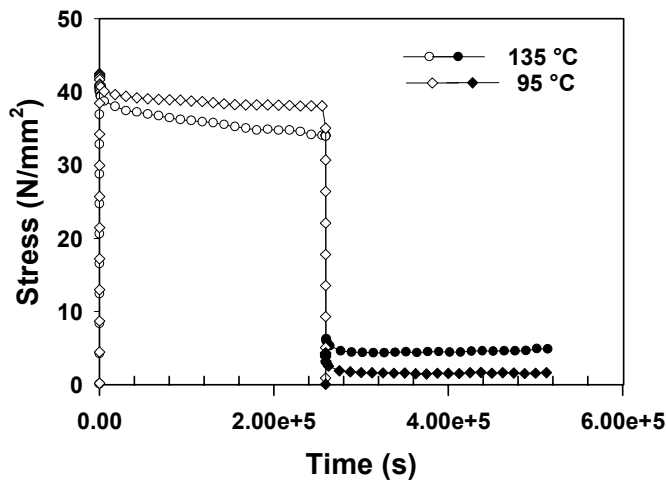


Figure 6.—Compressive stress relaxation at 95 and 135 °C as a function of time. Stress is plotted as absolute value, note that the sense of stress transposes during the recovery portion of the test so that filled symbols are tensile.

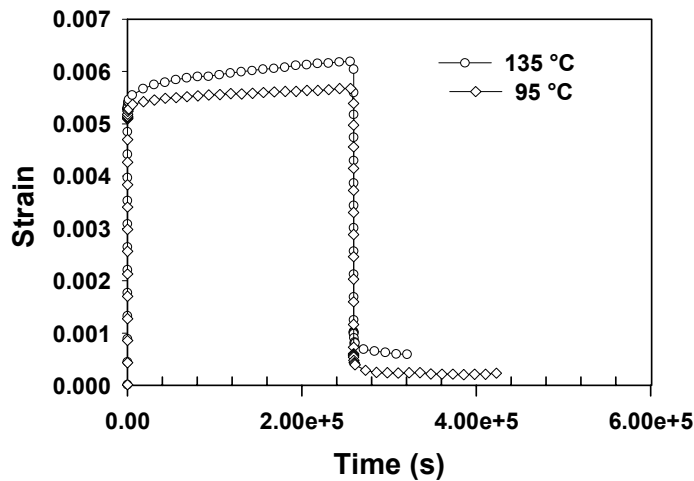


Figure 7.—Compressive creep at 95 and 135 °C as a function of time. Strain is plotted as absolute value.

95 °C. The horizontal distance, in Fig. 8, that the 135 °C curve is translated to overlap the 95 °C curve, is expressed as  $\log a_T$ . The term  $a_T$  is defined as the shift factor, the ratio of the time scale of the desired master curve to the time scale at an elevated temperature. In this case, the value for  $\log a_T$  was found to be 1.4. Confidence in the result is given by the apparent continuity of the overlapping shifted data (filled symbols) with the underlying 95 °C data. Thus the TTSP appears to be applicable in the time and temperature regime of these experiments.

The observations thus far raise some interesting issues with respect to constitutive model selection for flywheel simulation. First among them is the observation of stress/strain sign dependent material response raising the question of linearity and a recoverable zero stress-strain state. Turner [27] points out that the most practical definition for the term “non-linear” is when the stress at any particular time is not proportional to strain. Thus time

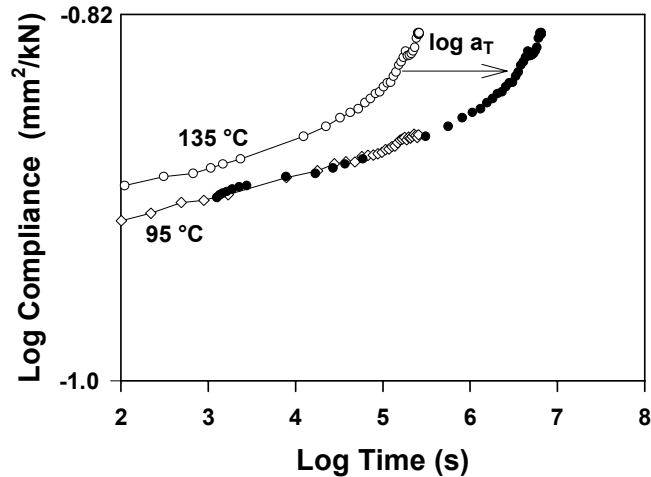


Figure 8.—Application of the time temperature superposition principle to compressive compliance data at 95 °C and 135 °C.  $\log a_T = 1.4$ , filled symbols are the shifted 135 °C data.

dependent compliance curves from tests made at different stress or strain levels should be identical for the material response to be linear.

Additional compressive stress relaxation and creep tests were made at 135 °C to examine the influence of load level on the response. The stress relaxation tests were made at  $-0.2\%$  and  $-0.8\%$  strain and the creep test was made at  $-68.9 \text{ N/mm}^2$ . The results of these tests and the previous compressive data at 135 °C are converted to time dependent compliance and plotted as a function of time in a logarithmic scale (Figure 9a). Time dependent compliance is defined here as the instantaneous ratio of strain to stress for both kinds of tests. Note that the compliance curve determined by the inverse of the relaxation modulus, as this definition implies, is not identical to the creep compliance; in the framework of a linear hereditary material, relaxation modulus and creep compliance are related by a convolution integral [18]. However for small strains they are approximately equal [28] as seen in Fig. 9.

The mean and standard deviation of compliance data as measured from the loading phase of these tests was determined to be  $0.128 \text{ mm}^2/\text{kN}$  and  $0.006 \text{ mm}^2/\text{kN}$ , respectively. The specimen-to-specimen variation in the initial compliance gives a sense of the expected variability of the time dependent compliance curves. This is illustrated in Fig. 9a. by attaching error bars corresponding to  $0.006 \text{ mm}^2/\text{kN}$  to a compliance curve near the median of the data. Note that the variation on repeat of the  $-0.5\%$  strain stress relaxation test is also of the same magnitude as the variation between the  $-0.2\%$  and the  $-0.8\%$  strain stress relaxation tests. The trend of increasing compressive compliance is repeated in all the compressive tests. The single representative compressive compliance curve with the error bars, from Figure 9a, is shown with compliance data from the tensile creep and tensile stress relaxation tests from Figures 4 and 5 (Figure 9b). It should be mentioned that these tensile compliance data have been compared to tensile compliance data provided by Raghavan and Meshii [20] for AS4/3501-6 carbon fiber reinforced epoxy. While there is an offset due to a difference in constituent properties and volume fraction, the slope of the AS4/3501-6 data and IM7/8552 were found to be similar over the common time frame of the two data sets.

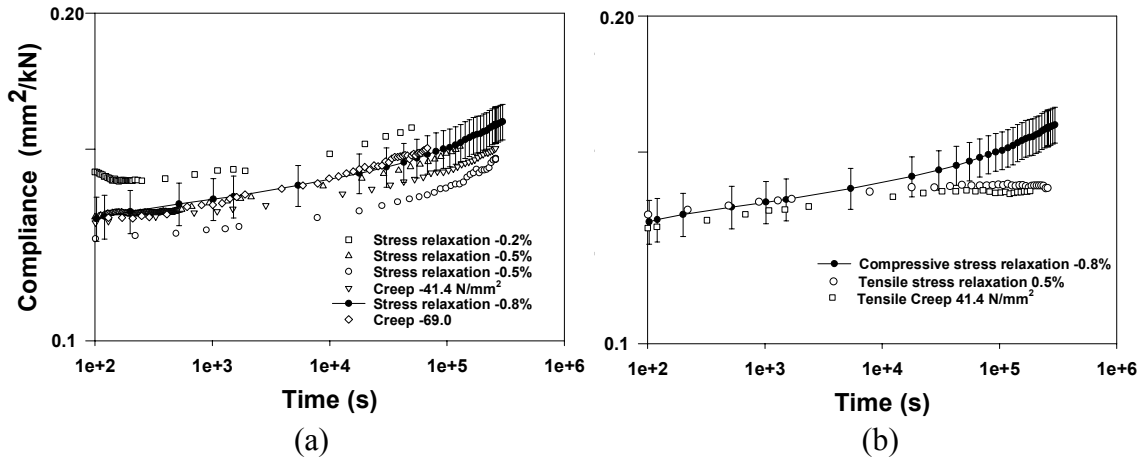


Figure 9.—Compliance from both creep and stress relaxation as a function of time on logarithmic axes for (a) compression and (b) compression and tension.

Figure 9a shows that for a particular range of time, these compression compliance data could be considered to be within the realm of linear behavior when accounting for specimen-to-specimen variability. Note however that acceptance tolerances for distinguishing between linear and non-linear responses when analyzing hereditary data do not seem to be established (see ASTM Standard Test Methods for Tensile, Compressive and Flexural Creep and Creep-Rupture of Plastics D-2990). In Fig. 9b, the two tensile compliance plots coincide closely with each other but begin to diverge from the representative compressive compliance after 10<sup>4</sup> s. As care was taken so that all specimens were prepared identically, their state of physical ageing may be presumed to be identical and therefore does not account for this behavior. Based on this observation, the use of the definition of a linear hereditary material and Boltzmann's principle of superposition for IM7/8552 becomes problematic if not intractable. This may be demonstrated further by an attempt to use Boltzmann's principle of superposition to determine the recovery phase of the data given in Figs. 5. Since the tensile relaxation response is nearly constant after 10<sup>4</sup> seconds, superposition of it on to the compressive relaxation response would predict near recovery of the zero stress state for both experiments. This result is only observed for the tensile relaxation test with a compressive recovery phase.

Clearly further investigation is needed to resolve this apparent paradox but it is believed that complex interactions on the microstructural level involving processing residual stresses can be an explanation. Micro-mechanical analysis and additional experiments are needed to verify this proposition. From an engineering perspective a sense of the weight of these issues may be given by reviewing the results of the prototypical fatigue test.

### *Prototypical Operational Loads*

The prototypical compressive fatigue cycle that was applied in these experiments had a mean stress of -41.4 N/mm<sup>2</sup>, a stress amplitude of 13.8 N/mm<sup>2</sup> and a triangular waveform. The period of each cycle was 60 s; the corresponding frequency was 0.017 Hz. Each experiment was 2.6 x 10<sup>5</sup>s (72 hrs) in duration. A test was made at 95 °C and at 135 °C. The data has been processed to provide extreme values of strain and the mean strain for each

sample cycle. The maximum, mean and minimum strains are plotted as a function of time in Fig. 10 for each test temperatures. The creep strain response for a compressive stress of  $-41.4 \text{ N/mm}^2$  is also shown in Fig. 10 for the corresponding test temperatures. The apparent mean strain of the fatigue response in Figs 10a and b closely matches the corresponding creep response. For this relatively harsh prototypical environment (operation cycle periods are likely to be much longer than 1 minute) synergistic loading effects are not present.

It appears that the relationship between the average strain response and the average applied fatigue stress is the same as that between the creep strain response and a constant compressive stress. Using the different tensile and compressive compliance curves in Fig. 9, it would be impossible to predict this result using Boltzmann's principle of superposition. For instance, the compliance curves of Fig. 9 would not predict zero creep strain for a fully reversed fatigue experiment. This would be a necessary result for the observations in Fig. 10 to be consistent with the definition of linear hereditary behavior.

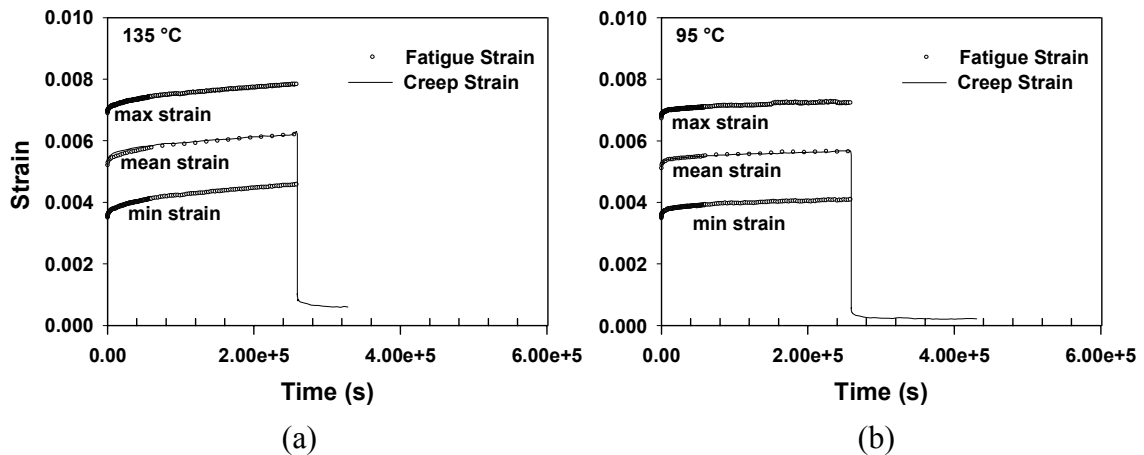


Figure 10.—Strain response in compressive fatigue compared to compressive creep data for a) test temperature  $135 \text{ }^\circ\text{C}$  and b) test temperature  $95 \text{ }^\circ\text{C}$ .

### Design Implications

There are several ramifications of these experimental results on the design of PMC flywheel rotors manufactured with a pre-load or strain-matching design. Experimentally this work examines the transverse response of the composite due to a controlled stress or strain boundary condition on uniaxial specimens. Under a controlled strain of  $-0.5\%$ , the stress relaxation was observed to be  $16.4\%$  after 72 hrs at  $135 \text{ }^\circ\text{C}$  in these uniaxial compression experiments. Fundamentally, within the strain, time and temperature regime of these tests, the compressive stress relaxation results can be viewed as an upper bound for the amount of relaxation that a radial pre-load would exhibit in a composite rotor. There are two primary reasons for this. First, some degree of radial compression will be maintained by the radial deflection of an elastic hub. Secondly, the relaxation response of a thin uniaxial specimen cannot be less than that of a rotor having any kind of lateral constraint. Obviously these two features can be controlled to minimize the impact of stress relaxation on radial pre-load. However, it is apparent from these experiments that any kind of design optimization or durability limit analysis requires having design data for the appropriate

loading mode. Using tensile constitutive data for IM7/8552 would have been non-conservative in any design analysis.

The difference between compressive and tensile time-temperature dependent material behavior could be problematic for designers wishing to assume a linear hereditary response. Although it may be possible to predict pressure losses in press fit rings fairly well (see e.g., Emerson and Bakis [10]), extending the analysis to cyclic loading situations would require a consideration for the possibility of sign dependent behavior in the composite. While comparisons of tensile and compressive time-temperature dependent behavior for composites are rare, those existing have reported differences between the two responses [13, 18]. These investigations and the experimental observations reported here point out the need for a more rigorous theoretical and experimental treatment of the time-temperature dependent behavior of PMCs.

Whenever designers face the need for long-term durability data there is an interest in accelerating the testing. Based on the available data there is an indication that TTSP may be used by the designer to generate long-term master curves using short-term data at elevated temperatures. Note that the study conducted here does not investigate the phenomenon of physical ageing which acts to slow the relaxation rate with time. Accordingly the master curves developed here would over predict the long-term relaxation. Struik [29] describes the appropriate test procedures and data reduction methods to account for physical aging; Gates and co-workers [18,19] have demonstrated these methods for PMCs.

## Summary and Conclusions

A series of experiments have been made to appraise the time-temperature response of filament wound IM7/8552 carbon fiber epoxy composite transverse to the reinforcing fiber. The polymer matrix composite is considered to be technology enabling rotor material in flywheel energy storage systems for space flight applications. Rotor designs utilizing the load carrying capacity of carbon fibers wound in the hoop direction are capable of high operational speeds and specific energies. Several design strategies obviate the problem of tensile radial stresses in the matrix-dominated direction through the introduction of compressive stress. Analytical work by Arnold and co-workers indicate that several transverse geometric parameters control the performance of these rotors. Therefore the safe-life qualification of PMCs for flywheel rotor applications may be limited by the time-temperature dependent behavior of the epoxy matrix in compression.

Filament wound specimen panels were made using the same manufacturing process as for polymer composite rotors. Flat coupon specimens were then cut from the panels parallel and perpendicular to the winding axis so that fibers were transverse and longitudinal to the loading direction. Compression and tensile testing was made at RT, 95 °C and 135 °C. The influence of strain rates from  $5 \times 10^{-6}/s$  to  $5 \times 10^{-3}/s$  was examined on the initial stress/strain response. Creep and stress relaxation response was studied over a 72 hr period. As anticipated, time-dependent effects are negligible when the load was applied parallel to the primary fiber direction. Loading perpendicular to the carbon fiber direction resulted in responses that were dependant on the sense of load and the test temperature. At 135 °C, compressive stresses relaxed 16.4% in 72 hrs under a fixed deformation of  $-0.5\%$  strain. Lowering test temperature to 95 °C reduced the extent of compressive stress relaxation to 13%. At a fixed tensile strain of 0.5% stresses relaxed only 7% in 72 hrs at 135°C. Designers of composite flywheel rotors may treat the compressive

stress relaxation data as an upper bound to the rate of pre-load relaxation. More accurate durability predictions require analyses such as those given by Saleeb and co-workers [1].

The time temperature superposition principle (TTSP) appears to be applicable for the time and temperature regimes of the test program. The shift factor to create a master curve at 95 °C was  $\log a_T = 1.4$ . The short time range data at 135 °C can be used to predict longer-term response at 95 °C. These curves do not account for physical aging so relaxation rates at longer times are likely to be overestimated [29]. Prototypical compression-compression fatigue tests exhibit a mean strain response that closely tracks the creep strain response for an “equivalent” creep test. The mean compression stress of the fatigue test was identical to the compression stress of the creep test.

Time dependent compliance data for tests made at different constant levels of strain or stress were found to nearly coincide if specimen to specimen variation is considered. However compression and tensile compliance data does not coincide. Consequently, the application of the definition of a linear hereditary material response and Boltzmann’s principle of superposition to describe the behavior of IM7/8552 in the regime of these experiments is problematic if not intractable. Undoubtedly microstructural analysis, including the influence of residual stresses due to processing, will be needed to resolve the paradoxes observed here for recovery and fatigue data. While limited, other comparisons of tensile and compressive time-temperature dependent data for composites report differences [13,18]. These findings support the need for more rigorous treatment of the influence sign dependency in a theoretical framework of PMC constitutive models.

## References

- [1] Saleeb, A.F., Arnold, S.M., and Al-Zoubi, N.R., “A Study of Time Dependent and Anisotropic Effects on the Deformation Response of Two Flywheel Rotor Designs” *Composite Materials: Testing and Design Fourteenth Volume, ASTM STP 1436*, C.E. Bakis, Ed., ASTM International, West Conshohocken, PA, 2003.
- [2] Genta, G., *Kinetic Energy Storage: Theory and Practice of Advanced Flywheel Systems*, Butterworths, 1985.
- [3] Keckler, C.R., Bechtel, R.T., and Groom, N.J., “An Assessment of Integrated Flywheel System Technology,” NASA CP 2346, 1984.
- [4] DeTeresa, S.J., “Materials for Advanced Flywheel Energy Storage Devices”, MRS Bulletin, 1999.
- [5] Bitterly, J.G., “Flywheel Technology,” IEEE AES Systems Magazine, 1998.
- [6] Arnold, S.M., A.F. Saleeb, and Al-Zoubi, N.R., “Deformation and Life of Composite Flywheel Disk and Multi-Disk Systems,” NASA/TM—2001-210578.
- [7] Tzeng, J.T., “Viscoelastic Analysis of Composite Flywheels for Energy Storage” ARL-TR-2610, U.S. Army Research Laboratory, Aberdeen Proving Ground, MD 21005.
- [8] Tzeng, J.T., “Viscoelastic Behavior of Composite Rotors at Elevated Temperatures” IEEE Transactions on Magnetics, Vol. 33, No. 1, 1997, pp. 413–418.
- [9] Emerson, R.P. and Bakis C.E., “Relaxation of Press-Fit Interference Pressure in Composite Flywheel Assemblies” Proc. 43th SAMPE Symposium and Exhibition, 31 May–June 4 1998, Long Beach, CA, SAMPE, Covina, CA 1998.

- [10] Emerson, R.P. and Bakis C.E., “Viscoelastic Behavior of Composite Flywheels” Proc. 45th SAMPE Symposium and Exhibition, 21–25 May 2000, Long Beach, CA, SAMPE, Covina, CA 2000.
- [11] Thompson, R.C., Pak, T.T., and Rech, B.M., “Hydroburst Test Methodology for Evaluation of Composite Structures” *Composite Materials: Testing and Design Fourteenth Volume, ASTM STP 1436*, C.E. Bakis, Ed., ASTM International, West Conshohocken, PA, 2003.
- [12] Irion, M.N., and Adams, D.F., "Compression Creep Testing of Unidirectional Composite Materials," *Composites*, Vol. 12, No. 2, April 1981, pp. 117–123.
- [13] Mohan, R., and Adams, D.F., "Nonlinear Creep-Recovery Response of a Polymer Matrix and Its Composites," *Experimental Mechanics*, Vol. 25, No. 3, September 1985, pp. 262–271.
- [14] Tuttle, M.E. and Brinson, H.F., “Prediction of the Long-Term Creep Compliance of General Composite Laminates” *Experimental Mechanics* March 1986, pp. 89–102.
- [15] Sullivan, J.L., “Measurement of Composite Creep” *Experimental Techniques* Sept./Oct. 1991, pp. 32–37.
- [16] Gates, T.S., “Experimental Characterization of Nonlinear, Rate-dependent Behavior in Advanced Polymer Composites” *Experimental Mechanics* March 1992, vol. 31, pp. 68–73.
- [17] Gates, T.S. and Sun, C.T., “Elastic/Viscoplastic Constitutive Model for Fiber Reinforced Thermoplastic Composites” *AIAA Journal*, vol. 29, No. 3, 1991 pp. 457–463.
- [18] Gates, T.S., Veazie, D.R. and Brinson, L.C. “A Comparison of Tension and Compression Creep in Polymeric Composite and the Effects of Physical Ageing on Creep” NASA TM 110273 August 1996, NASA Langley Research Center.
- [19] Brinson, L.C. and Gates, T.S., “Chapter 10—Viscoelasticity and Aging of Polymer Matrix Composites” *Comprehensive Composite Materials*. Editors in Chief, Kelly, A. and Zweben, C.H., Vol 2. 2000, pp. 333–368.
- [20] Raghavan, J. and Meshii, M., “Creep of Polymer Composites” *Composites Science and Technology* 57, 1997, pp. 1673–1688.
- [21] Al-Haik, M., Vaghar, M.R. Garmestani, H., and Shahawy, M., “Viscoplastic analysis of structural polymer composites using stress relaxation and creep data” *Composites Part B: engineering*, 32, 2001, pp. 165–170.
- [22] Arnold, S.M., Saleeb, A.F., and Castelli, M.G., “A General Time Dependent Constitutive Model: Part II—Application to a Titanium Alloy”, *Journal of Engineering Materials and Technology*, 122, pp. 1–9.
- [23] Hexcel Advanced Composite Materials Technical Literature, "Hexcel 8552 Epoxy Matrix - Product Data," Hexcel, 5794 West Las Positas Blvd., P.O. Box 8181, Pleasanton, CA 94588-8781, August, 1998.
- [24] Baaklini, G.Y., Kono, K.K., Martin, R.E., and Thompson, R., “NDE Methodologies for Composite Flywheels Certification,” SAE Conference, 2000 Power Systems, San Diego October-November 2000. (also NASA/TM—2000-210473, October 2000).

- [25] Perry, C.C., “Strain-Gage Reinforcement Effects on Low Modulus Materials-Section IIID,” *Manual on Experimental Methods for Mechanical Testing of Composites*, Ed. M.E. Tuttle and R.L. Pendleton, SEM (1989).
- [26] Perry, C.C., “Strain-Gage Reinforcement Effects on Orthotropic Materials-Section IIID,” *Manual on Experimental Methods for Mechanical Testing of Composites*, Ed. M.E. Tuttle and R.L. Pendleton, SEM (1989).
- [27] Turner, S. Chapter 4 “Creep in Glassy Polymers” in *The Physics of Glassy Polymers* ed. R.N. Haward, Applied Science Publishers LTD, London, 1973
- [28] Suh, N.S. and Turner, A.P.L., *Elements of the Mechanical Behavior of Solids*, 1974, Scripta Book Co., Washington D.C. p. 314.
- [29] Struik, L.C.E. *Physical Aging in Amorphous Polymers and Other Materials*, 1978, Elsevier Scientific Publishing Co. Amsterdam, Netherlands.

# REPORT DOCUMENTATION PAGE

*Form Approved*  
*OMB No. 0704-0188*

Public reporting burden for this collection of information is estimated to average 1 hour per response, including the time for reviewing instructions, searching existing data sources, gathering and maintaining the data needed, and completing and reviewing the collection of information. Send comments regarding this burden estimate or any other aspect of this collection of information, including suggestions for reducing this burden, to Washington Headquarters Services, Directorate for Information Operations and Reports, 1215 Jefferson Davis Highway, Suite 1204, Arlington, VA 22202-4302, and to the Office of Management and Budget, Paperwork Reduction Project (0704-0188), Washington, DC 20503.

<b>1. AGENCY USE ONLY</b> ( <i>Leave blank</i> )	<b>2. REPORT DATE</b> January 2004	<b>3. REPORT TYPE AND DATES COVERED</b> Technical Memorandum	
<b>4. TITLE AND SUBTITLE</b>  Time-Temperature Dependent Response of Filament Wound Composites for Flywheel Rotors		<b>5. FUNDING NUMBERS</b>  WBS-22-755-12-11	
<b>6. AUTHOR(S)</b>  John C. Thesken, Cheryl L. Bowman, Steven M. Arnold, and Richard C. Thompson			
<b>7. PERFORMING ORGANIZATION NAME(S) AND ADDRESS(ES)</b>  National Aeronautics and Space Administration John H. Glenn Research Center at Lewis Field Cleveland, Ohio 44135-3191		<b>8. PERFORMING ORGANIZATION REPORT NUMBER</b>  E-13757	
<b>9. SPONSORING/MONITORING AGENCY NAME(S) AND ADDRESS(ES)</b>  National Aeronautics and Space Administration Washington, DC 20546-0001		<b>10. SPONSORING/MONITORING AGENCY REPORT NUMBER</b>  NASA TM-2004-212102	
<b>11. SUPPLEMENTARY NOTES</b> Prepared for the 14th Symposium on Composite Materials: Testing and Design sponsored by the American Society for Testing and Materials, Pittsburgh, Pennsylvania, March 11-12, 2002. John C. Thesken, Ohio Aerospace Institute, Brook Park, Ohio 44142; Cheryl L. Bowman and Steven M. Arnold, NASA Glenn Research Center; Richard C. Thompson, University of Texas at Austin, Austin, Texas 78712. Responsible person, John C. Thesken, organization code 5920, 216-433-3012.			
<b>12a. DISTRIBUTION/AVAILABILITY STATEMENT</b>  Unclassified - Unlimited Subject Category: 39  Available electronically at <a href="http://gltrs.grc.nasa.gov">http://gltrs.grc.nasa.gov</a> This publication is available from the NASA Center for AeroSpace Information, 301-621-0390.		<b>12b. DISTRIBUTION CODE</b>	
<b>13. ABSTRACT</b> ( <i>Maximum 200 words</i> )  Flywheel energy storage offers an attractive alternative to battery systems used in space applications such as the International Space Station. Rotor designs capable of high specific energies benefit from the load carrying capacity of hoop wound carbon fibers but their long-term durability may be limited by time-temperature dependent radial deformations. This was investigated for the carbon/epoxy rotor material, IM7/8552. Coupon specimens were sectioned from filament wound panels. These were tested in compression and tension at room temperature (RT), 95 and 135 °C for strain rates from $5 \times 10^{-6}/s$ to $5 \times 10^{-3}/s$ . Time, temperature and load sign dependent effects were significant transverse to the fiber. At -0.5 percent strain for 72 hr, compressive stresses relaxed 16.4 percent at 135 °C and 13 percent at 95 °C. Tensile stresses relaxed only 7 percent in 72 hr at 135 °C for 0.5 percent strain. Using linear hereditary material response and Boltzmann's principle of superposition to describe this behavior is problematic if not intractable. Micromechanics analysis including the effects of processing residual stresses is needed to resolve the paradoxes. Uniaxial compressive stress relaxation data may be used to bound the loss of radial pre-load stresses in flywheel rotors.			
<b>14. SUBJECT TERMS</b>  IM7/8552; Carbon fiber epoxy composite; Filament wound flywheel; Creep; Stress relaxation; Linear hereditary; Time-temperature; Load sign effects		<b>15. NUMBER OF PAGES</b> 25	
		<b>16. PRICE CODE</b>	
<b>17. SECURITY CLASSIFICATION OF REPORT</b> Unclassified	<b>18. SECURITY CLASSIFICATION OF THIS PAGE</b> Unclassified	<b>19. SECURITY CLASSIFICATION OF ABSTRACT</b> Unclassified	<b>20. LIMITATION OF ABSTRACT</b>